

AD-A210 986

AD

TECHNICAL REPORT ARCCB-TR-89016

**FRACTURE AND THREE-DIMENSIONAL STRESS ANALYSES OF 7075 ALUMINUM PROJECTILE COMPONENTS UNDER SPIN AND INERTIA LOAD**

J. H. UNDERWOOD

G. P. O'HARA

M. A. SCAVULLO

B. A. KONRAD

JUNE 1989

DTIC  
ELECTE  
AUG 8 1989  
S B D



US ARMY ARMAMENT RESEARCH,  
DEVELOPMENT AND ENGINEERING CENTER  
CLOSE COMBAT ARMAMENTS CENTER  
BENÉT LABORATORIES  
WATERVLIET, N.Y. 12189-4050



APPROVED FOR PUBLIC RELEASE; DISTRIBUTION UNLIMITED

1 07 1 46

#### DISCLAIMER

The findings in this report are not to be construed as an official Department of the Army position unless so designated by other authorized documents.

The use of trade name(s) and/or manufacturer(s) does not constitute an official indorsement or approval.

#### DESTRUCTION NOTICE

For classified documents, follow the procedures in DoD 5200.22-M, Industrial Security Manual, Section II-19 or DoD 5200.1-R, Information Security Program Regulation, Chapter IX.

For unclassified, limited documents, destroy by any method that will prevent disclosure of contents or reconstruction of the document.

For unclassified, unlimited documents, destroy when the report is no longer needed. Do not return it to the originator.



7. AUTHORS (Cont'd)

B. A. Konrad  
 U.S. Army ARDEC  
 Close Combat Armaments Center  
 Tank Ammunition Branch B  
 Picatinny Arsenal, NJ 07806-5000

20. ABSTRACT (Cont'd)

specifications which could prevent failures in the future. An energy-to-failure test similar to the Charpy test was found to be the most discriminating.



<b>Accession For</b>	
NTIS GRA&I	<input checked="" type="checkbox"/>
DTIC TAB	<input type="checkbox"/>
Unannounced	<input type="checkbox"/>
Justification	
By _____	
Distribution/	
Availability Codes	
Dist	Avail and/or Special
A-1	

UNCLASSIFIED

## TABLE OF CONTENTS

	<u>Page</u>
ACKNOWLEDGEMENTS .....	iii
BACKGROUND .....	1
PROBLEM .....	4
STRESS ANALYSIS .....	4
MATERIAL .....	9
Tensile Mechanical Tests .....	9
Fracture Toughness Tests .....	10
Notched-Bend Energy Tests .....	11
SOLUTION .....	13
Design Change .....	13
Material Change .....	14
SUMMARY .....	16
REFERENCES .....	17

### TABLES

I. TENSILE MECHANICAL PROPERTIES OF 7075-T6 ALUMINUM SABOTS WHICH EXPERIENCED FAILURE; MEAN VALUES OF THREE OR MORE REPEAT TESTS .....	9
II. PLANE-STRAIN FRACTURE TOUGHNESS OF 7075-T6 ALUMINUM SABOTS WHICH EXPERIENCED FAILURE; UNITS of MPa $m^{1/2}$ .....	11
III. SLOW NOTCHED-BEND ENERGY OF 7075-T6 ALUMINUM SABOTS WHICH EXPERIENCED FAILURE; UNITS OF J .....	13

### LIST OF ILLUSTRATIONS

1. Finite element model of a long rod and interconnecting sabot with service loading indicated .....	2
2. Sketch of sabot segment with three types of test specimen shown .....	3

3. Contours of maximum principal stress for rod and sabot with a tube pressure of 410 MPa and no spin .....	7
4. Contours of maximum principal stress for rod and sabot at tube exit with a tube pressure of 70 MPa and a spin rate of 300 Hz .....	8
5. Sketch of slow notched-bend energy test arrangement and typical load versus load-line displacement plot .....	12

## ACKNOWLEDGEMENTS

We are pleased to acknowledge the help of J. T. Ritter and M. T. Butler of Materials Research Laboratories in preparing this report.

## BACKGROUND

This study involves a cannon-launched kinetic energy projectile which has two basic components: a slender cylindrical rod and a discarding sabot. A portion of such a projectile is shown in Figure 1, the finite element grid used to model the projectile and its loading. The rod is made of a heavy metal, such as tungsten or uranium, to produce a high kinetic energy. The sabot is of a light material, usually aluminum, so that it uses as little of the energy intended for the rod as possible.

The sabot attaches to and accelerates the rod within the cannon, and once clear of the tube, it separates into three 120-degree segments. The sabot is attached to the rod via annular interconnecting lugs on the outer radius of the rod and the inner radius of the sabot as shown in Figure 2. After separation from the rod, the sabot segments decelerate rapidly and the rod continues on as the kinetic energy projectile.

A fracture problem previously experienced with this type of projectile was the brittle failure of the rod during peak acceleration in the cannon (ref 1). The inertial stresses due to acceleration were concentrated by the notch effect of the lugs on the rod, and failure resulted. The present problem with the sabot apparently occurred during a different part of the cannon launch process after the peak acceleration occurred.

<sup>1</sup>J. H. Underwood and M. A. Scavullo, "Fracture Behavior of a Uranium or Tungsten Alloy Notched Component With Inertia Loading," Fracture Mechanics: Sixteenth Symposium, ASTM STP 868, (M. F. Kanninen and A. T. Hopper, eds.), American Society for Testing and Materials, Philadelphia, PA, 1985, pp. 554-568.

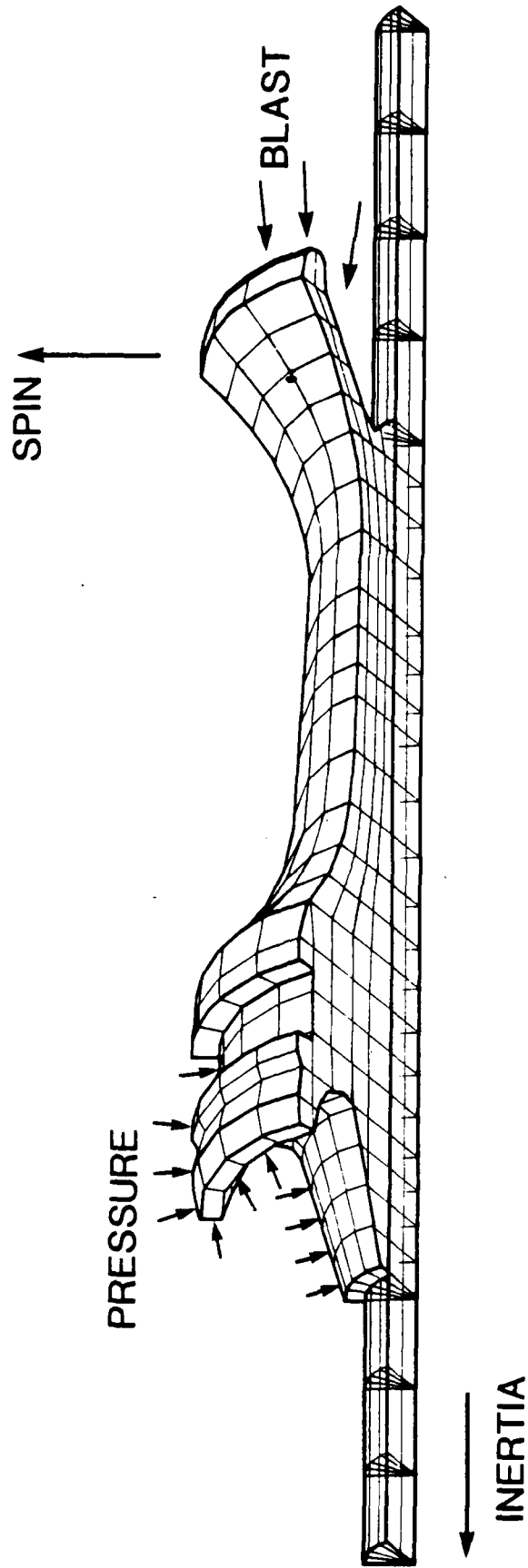


Figure 1. Finite element model of a long rod and interconnecting sabot with service loading indicated.

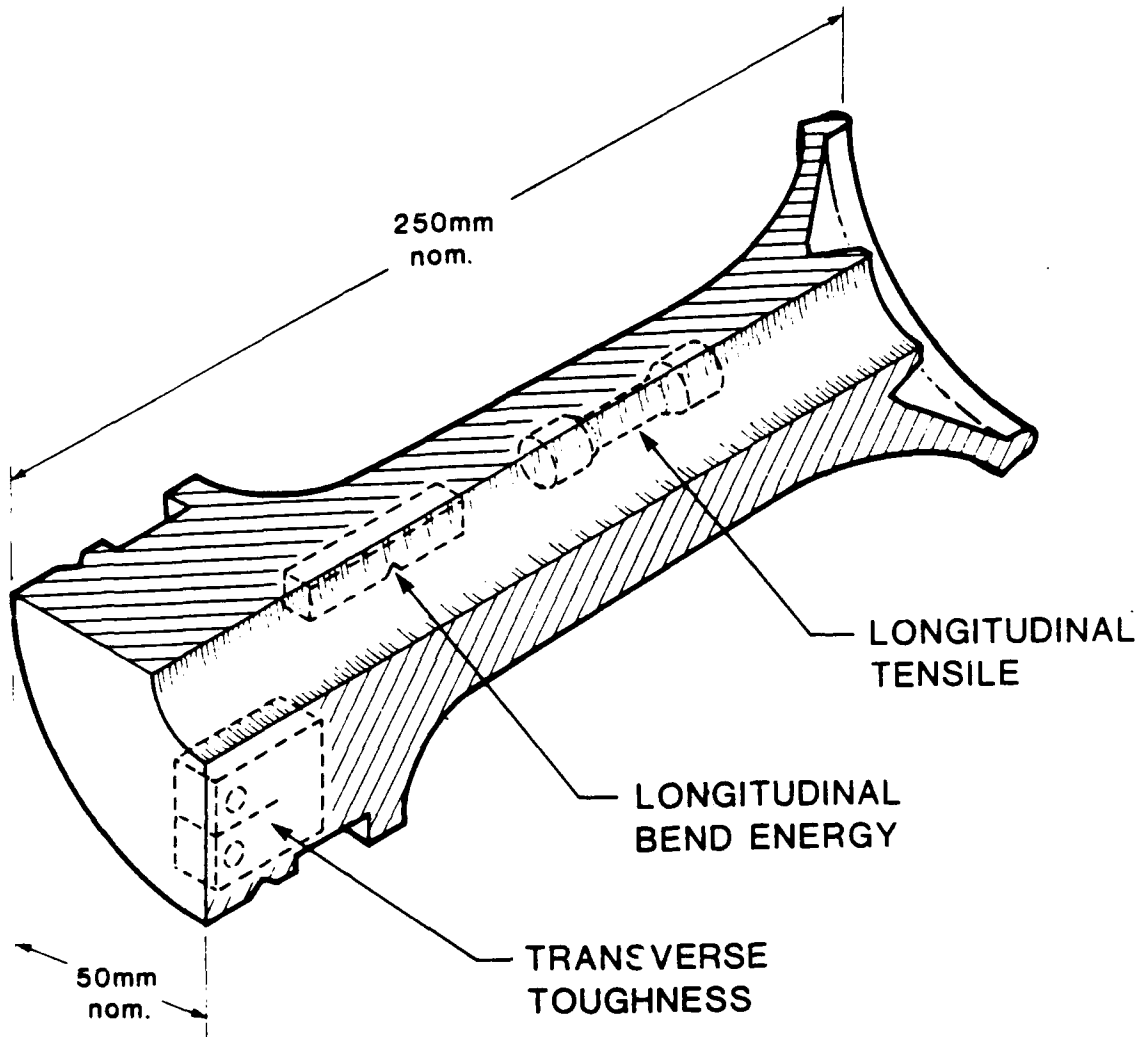


Figure 2. Sketch of sabot segment with three types of test specimen shown.

## PROBLEM

The present fracture problem is that occasionally one or more sabot segments suffered a brittle fracture and fragmentation, sometimes into several dozen pieces. The fragmentation failures often affected the flight direction of the rod and sometimes its velocity, therefore they had to be prevented. Initially, failures were noted with projectiles from one of the two manufacturers, indicated as supplier number 1 in Tables I, II, and III. Subsequently, fragmentation failures were observed during the launch of projectiles supplied by both manufacturers, primarily when the projectiles were preconditioned and launched at low temperature,  $-40^{\circ}\text{C}$ . The sabot material is a 7075-T6 aluminum extrusion, a material generally not used for fracture critical applications. However, this material clearly met the basic requirement of a high ratio of strength-to-weight, and the need for a fracture-resistant material was not readily apparent until the present spate of failures.

Eventually, the fragmentation failures became sufficiently recurrent to initiate a failure investigation. Highlights of the investigation are described here, with emphasis on the three-dimensional finite element stress analysis of the projectile under service loads and the fracture mechanics testing and analysis performed on the sabot material.

## STRESS ANALYSIS

Figure 1 shows the three-dimensional finite element grid used to identify the service loads which caused the failures. Initially, a two-dimensional analysis was performed as in Reference 1. The failure experience with the

<sup>1</sup>J. H. Underwood and M. A. Scavullo, "Fracture Behavior of a Uranium or Tungsten Alloy Notched Component With Inertia Loading," Fracture Mechanics: Sixteenth Symposium, ASTM STP 868, (M. F. Kanninen and A. T. Hopper, eds.), American Society for Testing and Materials, Philadelphia, PA, 1985, pp. 554-568.

sabots was sporadic, indicating that service loading conditions sometimes combined to cause failure and sometimes did not, calling for more stress details, and hence the three-dimensional analysis. In addition, features of the sabot geometry led to clearly non-axisymmetric stresses. For example, one key feature was the segmentation of the sabot; no tensile stress and little shear stress can be present on the mating surfaces of the segments, and this cannot be modelled in two dimensions.

The three-dimensional analysis used high order brick elements and included the appropriately different elastic moduli and densities for the aluminum sabot and uranium rod. The elements which modelled the attachment between the sabot and rod included the special boundary conditions of the lug interconnection. For example, significant axial load was allowed between the two components, but radial tension was not.

The various types of service loading on the sabot are indicated in Figure 1. The highest pressure and inertia loads occur relatively early in the launch process when the projectile is near its starting position at the breech end of the cannon. The centrifugal loads due to spin and the aerodynamic blast loads are most significant as the projectile leaves the muzzle of the cannon tube. The spin is imparted to the projectile by a nylon band which follows the twist of the cannon rifling and thereby applies a torque to the projectile by way of sliding friction between the band and the sabot. The band fits into the rectangularly shaped groove in the outer surface of the sabot (Figures 1 and 2) and also serves as a pressure seal.

Finite element calculations were performed to model combinations of the various service loadings. Two loading situations are particularly important, one in which the sabot stresses are generally compressive for a significant

portion of the launch process, and one which shows high values of tensile stress. Figure 3 is a contour plot of maximum principal stress for a model of the projectile near the beginning of the launch process at the maximum cannon pressure of a typical launch. As the projectile begins to move down the tube, the cannon pressure and the generally compressive stress in the sabot progressively diminish. The overall result is that while the projectile is in the tube, no significant tensile stresses develop in the sabot which could cause a failure. The reason for the lack of tensile stresses is the compression-stress effect of the cannon pressure on the sabot which is restrained from significant deformation by the rod and the tube. Note in Figure 3 that the compressive stresses in the sabot are at the same general level as the tube pressure.

Figure 4 shows the maximum principal stresses in the projectile as it leaves the tube. At this point in a typical launch, a tube pressure of about 70 MPa would still be applied to the rear of the sabot. In addition, a spin rate of 300 Hz was included in the model based on spin measurements from a group of projectiles which experienced some failures. A comparison of Figures 3 and 4 shows marked differences, particularly at two locations. The stress in Figure 4 at the root of the large radius at the rear of the sabot changed from compression to tension, a tensile stress which is significantly above the yield strength of the aluminum (see Table I). A second location at which the stress changed from compression to tension as the projectile exits the tube is the so-called saddle area, toward the front of the sabot. The bottom surface of the saddle contains yield-level tensile stresses, due to the bending which is allowed because the sabot is no longer restrained by the tube. It is this bending, a result of the unrestrained spin stresses in the sabot, which is believed to be the primary cause of the fragmentation failures. The failures

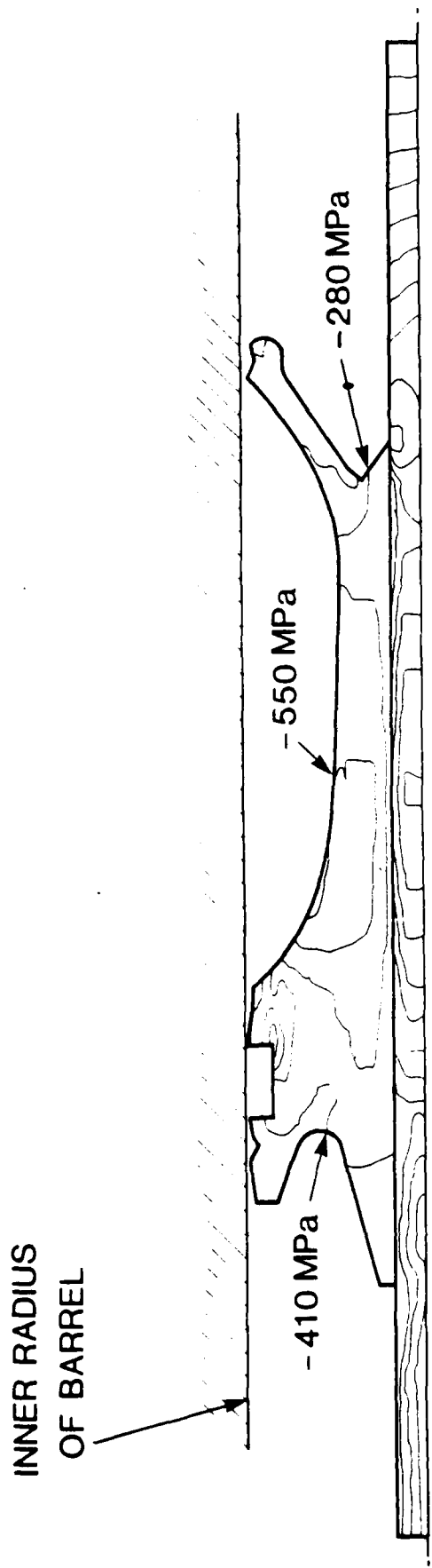


Figure 3. Contours of maximum principal stress for rod and sabot with a tube pressure of 410 MPa and no spin.

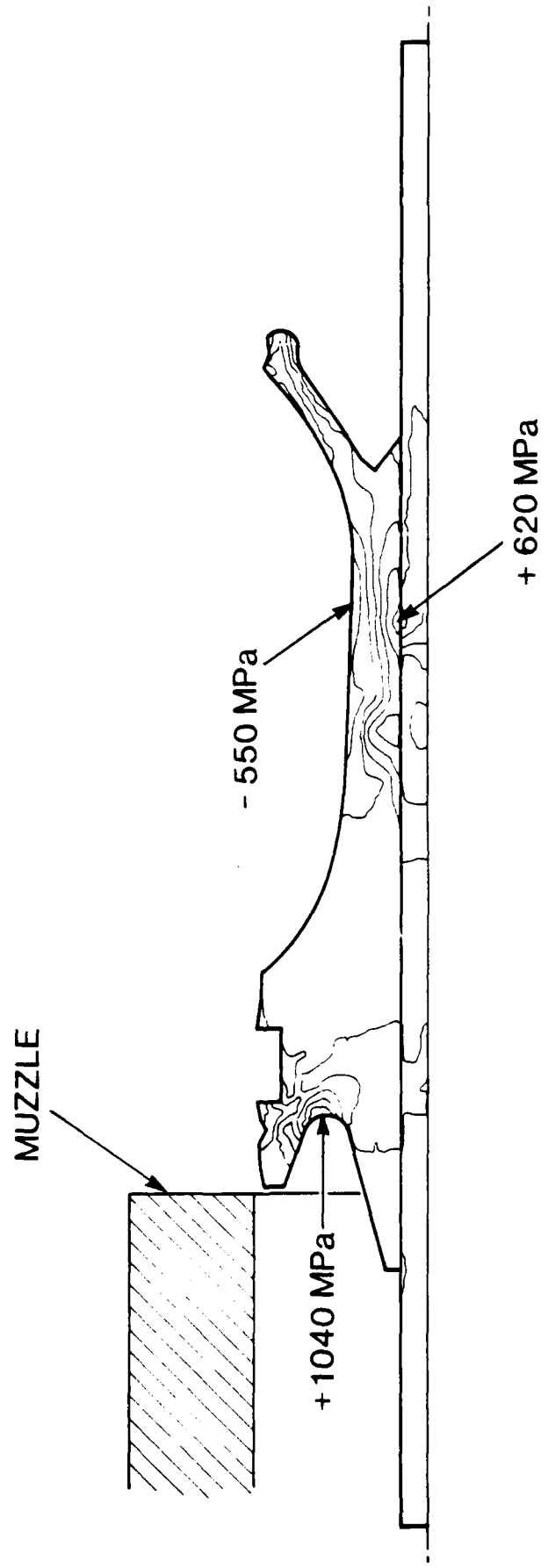


Figure 4. Contours of maximum principal stress for rod and sabot at tube exit with a tube pressure of 70 MPa and a spin rate of 300 Hz.

initiated at the sabot lug fillets, where the tensile bending stress is increased further by the stress-concentration effect of the lugs.

## MATERIAL

### Tensile Mechanical Tests

A range of mechanical and fracture testing of the sabot material was undertaken for two purposes. First, since the failures were sporadic, an attempt was made to find a test which could separate good material from bad in projectiles already in production. Second, the test results could also be used to change the material specification for subsequent sabot production. At the time of the failures the sabot specification was 7075-T6 aluminum with a minimum, longitudinal-direction, room temperature yield strength of 560 MPa. Table I gives the tensile mechanical test results, which show that all materials met the specification and there was no significant difference in tensile properties of

**TABLE I. TENSILE MECHANICAL PROPERTIES OF 7075-T6 ALUMINUM SABOTS WHICH EXPERIENCED FAILURE; MEAN VALUES OF THREE OR MORE REPEAT TESTS**

Test Temperature Supplier	Longitudinal Orientation				Short Transverse Orientation			
	+21°C		-40°C		+21°C		-40°C	
	#1	#2	#1	#2	#1	#2	#1	#2
Yield Strength 0.2% offset; MPa	616	613	634	642	499	546	520	489
Ultimate Strength; MPa	658	664	675	686	555	598	573	560
Elongation; %	9.3	10.5	8.4	8.4	8.7	10.3	6.4	5.3
Reduction-in-Area; %	14.0	13.7	9.4	10.3	10.7	14.4	7.7	6.4

the two materials. A test result would be considered different if the difference between the means of a set of results was greater than the larger standard deviation

$$| \text{mean \#1} - \text{mean \#2} | > \text{larger standard deviation} \quad (1)$$

Of the 16 sets of results in Table I comparing tensile results from the two suppliers, only the short transverse yield and ultimate strengths showed a difference in mean greater than the standard deviation. However, note the lack of consistency. At +21°C, material #2 was the higher strength, whereas at -40°C, #1 was stronger. One consistent result of the tensile tests was short transverse strengths considerably lower than longitudinal strengths. This is expected for high strength aluminum extrusions (ref 2).

#### Fracture Toughness Tests

Plane-strain fracture toughness  $K_{IC}$  tests were performed for the sabot materials. Although a  $K_{IC}$  value was not specified for the sabot nor is one usually specified for 7075-T6 aluminum, it is nevertheless an appropriate selection for an investigation of fragmentation failure. In most cases, the  $K_{IC}$  results (Table II) satisfied the specimen minimum thickness and width criteria of ASTM Standard E-399 (ref 3). The exception was the width of the longitudinal specimens, being from 60 to 75 percent of the required minimum. The  $K_{IC}$  values of both materials were in the expected range for 7075-T6 (ref 2). However, there was some indication that  $K_{IC}$  could separate the two materials. The short transverse  $K_{IC}$  results gave a difference of mean significantly greater than the

<sup>2</sup>R. J. Bucci, "Selecting Aluminum Alloys to Resist Failure by Fracture Mechanisms," Engineering Fracture Mechanics, Vol. 12, 1979, pp. 407-441.

<sup>3</sup>"Standard Test Method for Plane-Strain Fracture Toughness of Metallic Materials, ASTM E-399," 1986 Annual Book of ASTM Standards, Vol. 03.01, American Society for Testing and Materials, Philadelphia, PA, 1986, pp. 522-557.

TABLE II. PLANE-STRAIN FRACTURE TOUGHNESS OF 7075-T6 ALUMINUM SABOTS WHICH EXPERIENCED FAILURE; UNITS of MPa  $m^{1/2}$

Test Temperature	Fracture Toughness, Longitudinal (L-R)				Fracture Toughness, Short Transverse (R-L)			
	+21°C		-40°C		+21°C		-40°C	
Supplier	#1	#2	#1	#2	#1	#2	#1	#2
Number of Repeats	8	4	8	4	6	2	8	4
Standard Deviation	1.8	3.3	3.2	3.2	2.2	2.6	1.4	1.7
Mean Value	32.6	35.6	32.7	34.7	21.1	25.0	18.9	23.4

standard deviations for both the +21°C and -40°C results. Note also the particularly low value of short transverse fracture toughness for the conditions in which failure was most prevalent, material #1 at -40°C.

#### Notched-Bend Energy Tests

The partial success of fracture toughness in differentiating between the materials led to tests of notched-bend energy. This approach was successfully used in prior work, albeit with different materials (ref 1). Figure 5 outlines the test arrangement and concept. A specimen similar to the Charpy specimen of ASTM Standard E-23 (ref 4) was loaded slowly to failure, that is, with about ten seconds from zero to failure load. The specimen deflection measured near the notch was used to calculate the deflection of the specimen along the load line,  $\delta_{LL}$ , as

$$\delta_{LL} = \delta S/2 \quad (2)$$

<sup>1</sup>J. H. Underwood and M. A. Scavullo, "Fracture Behavior of a Uranium or Tungsten Alloy Notched Component With Inertia Loading," Fracture Mechanics: Sixteenth Symposium, ASTM STP 868, (M. F. Kanninen and A. T. Hopper, eds.), American Society for Testing and Materials, Philadelphia, PA, 1985, pp. 554-568.

<sup>4</sup>"Standard Methods for Notched Bar Impact Testing of Metallic Materials, ASTM E-23," 1986 Annual Book of ASTM Standards, Vol. 03.01, American Society for Testing and Materials, Philadelphia, PA, pp. 229-253.

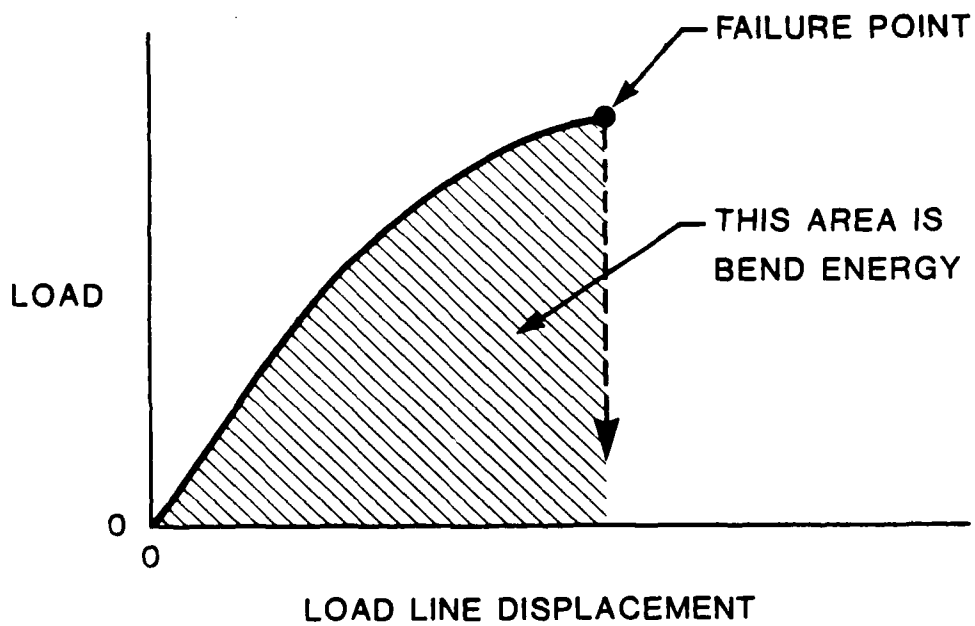
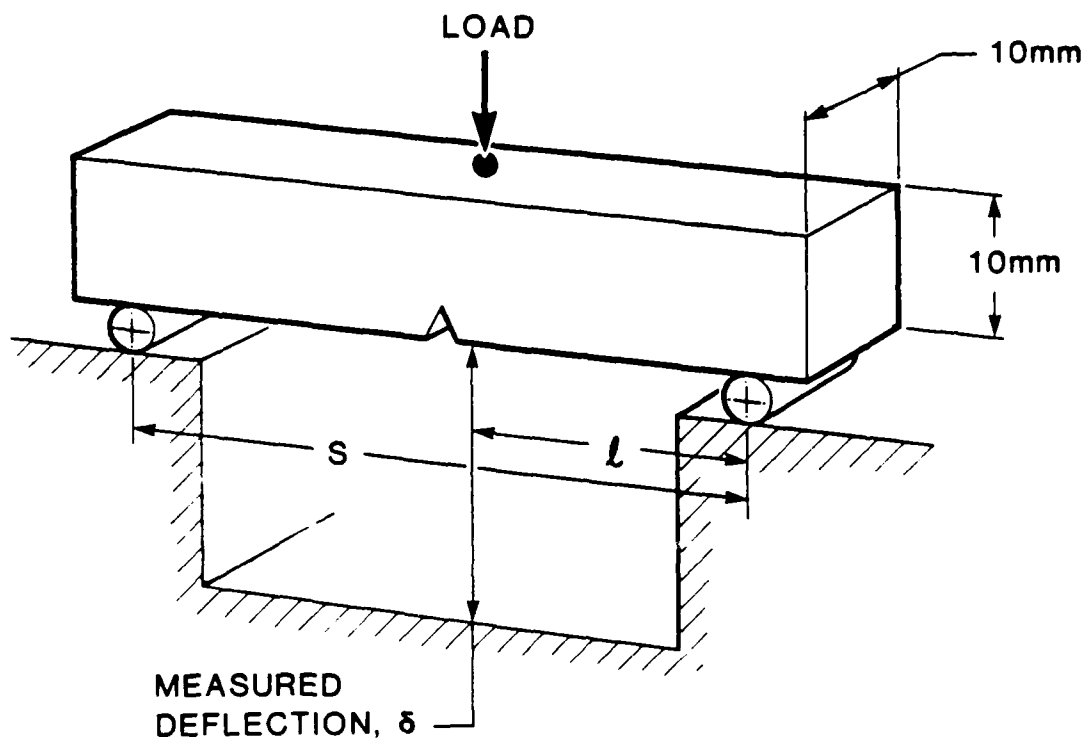


Figure 5. Sketch of slow notched-bend energy test arrangement, above, and typical load versus load-line displacement plot, below.

The load-line deflection was used to obtain the total strain energy-to-failure, which apart from the slower loading, is similar to the energy in a Charpy impact test. The results, as shown in Table III, were affected by a difference in the test specimens. The sabot dimensions in the radial direction required a support span,  $S = 30$  mm for the short transverse specimens, smaller than the  $S = 40$  mm used for the longitudinal specimens. This is believed to have reduced the total strain energy in the short transverse tests by a given amount due to a smaller elastic strain energy-to-failure for the shorter span. The important finding of the notched-bend energy tests was that all of the results yielded a difference of mean significantly greater than the standard deviations.

TABLE III. SLOW NOTCHED-BEND ENERGY OF 7075-T6 ALUMINUM SABOTS WHICH EXPERIENCED FAILURE; UNITS OF J

Test Temperature	Bend Energy, Longitudinal (L-R)				Bend Energy, Short Transverse (R-L)			
	+21°C		-40°C		+21°C		-40°C	
	#1	#2	#1	#2	#1	#2	#1	#2
Supplier								
Number of Repeats	7	4	8	4	8	4	8	2
Standard Deviation	0.21	0.41	0.37	0.31	0.34	0.32	0.19	0.07
Mean Value	4.25	5.50	3.24	4.61	2.40	3.27	2.17	2.71

## SOLUTION

### Design Change

The short-term solution to the fragmentation problem was a design change to the nylon band, a reduction in the interference between the band and the gap formed between the tube and the sabot. The reduced interference lowered the

sliding friction between the band and sabot, thus lowering the spin rate of the projectile. A rate of about 100 Hz was typically measured following the design change. Since centrifugal loads vary as the square of angular velocity (ref 5), a reduction from 300 to 100 Hz would result in a ninefold reduction of the tensile stress related to spin. The value of +620 MPa tensile stress, discussed in relation to Figure 4, would be reduced to about +70 MPa. Immediately following the band design change, the incidence of sabot fragmentation failures dropped to a small fraction of the former level.

### Material Change

The significantly reduced incidence of failures removed the urgency for a change in material for the projectiles under consideration. However, long-term recommendations were made regarding sabot material specifications for future projectile designs. The general recommendation was to replace the very high strength 7075-T6 material with a slightly lower strength material which also has a specified minimum fracture toughness. An alloy of the 7050-T7 type was suggested, provided that extrusions of the required size were available. Controlled low levels of iron and silicon combined with the overaged T7 condition have resulted in a useful combination of high strength and toughness in this type of aluminum alloy, with typical short transverse fracture toughness of 26 MPa m<sup>1/2</sup>, compared with 21 MPa m<sup>1/2</sup> for 7075-T6 (ref 2). The associated loss of even a small amount of strength requires careful consideration because of the generally high level of launch stresses in this type of projectile. However, a slightly lower strength, higher toughness material was considered the best means

<sup>2</sup>R. J. Bucci, "Selecting Aluminum Alloys to Resist Failure by Fracture Mechanisms," Engineering Fracture Mechanics, Vol. 12, 1979, pp. 407-441.

<sup>5</sup>R. J. Roark and W. C. Young, Formulas for Stress and Strain, McGraw-Hill Book Company, New York, 1975, pp. 564-567.

to avoid fragmentation type failures in future projectile designs. A 7050-T7 type material is also known to have significantly higher resistance to stress-corrosion cracking than 7075-T6 (ref 2). This failure mode must be considered for any projectiles which are stored for long periods before use.

The results of the investigation were also used to recommend a fracture toughness screening test, simpler than the  $K_{IC}$  test, but still a good indicator of fracture toughness. None of the tensile mechanical tests could differentiate between two materials with different failure incidences, so tensile tests would not be expected to be an effective indicator of fracture toughness. A similar result was obtained for steel forgings (ref 6). The notched-bend energy test, which clearly discriminated between the two materials, was recommended as a screening test. It is similar to the tear resistance test used for aluminum alloys (ref 2), and it is particularly well-suited to the sabot in two areas. First, the test is bending stress-controlled, as is the failure of the sabot, and second, the root radius of the Charpy specimen notch is 0.25 mm, the same as the radius of the sabot lug fillets. Because of these similarities between the bend energy test and the service conditions, the relatively simple test gave a good description of the fracture of the projectile component.

Finally, it is emphasized that although both the  $K_{IC}$  and bend energy tests can successfully separate the two materials, the bend energy is the better separator (Tables II and III). This is because the  $K_{IC}$  test measures resistance to growth of a pre-existing crack, whereas the notched-bend energy test measures

<sup>2</sup>R. J. Bucci, "Selecting Aluminum Alloys to Resist Failure by Fracture Mechanisms," Engineering Fracture Mechanics, Vol. 12, 1979, pp. 407-441.

<sup>6</sup>J. H. Underwood and G. S. Leger, "Fracture Toughness of High Strength Steel Predicted from Charpy Energy or Reduction in Area," Fracture Mechanics: Fifteenth Symposium, ASTM STP 833, (R. J. Sanford, ed.), American Society for Testing and Materials, Philadelphia, PA, 1984, pp. 481-498.

resistance to initiation of a crack at a notch root. Since the sabot failures were controlled by initiation of cracks at the lug fillets, the notched-bend energy test would be expected to be the more discriminating. However, the  $K_{Ic}$  test has the advantages of being more widely used and, when required, can be used for allowed-defect size and design calculations.

#### SUMMARY

The following key points can be derived from the case study of the 7075-T6 aluminum sabot.

1. The primary cause of the failures was the centrifugal bending stresses in the sabot which occurred just after exit from the tube, when the restraint supplied by the tube was lost. A design change which lowered the spin rate greatly reduced the failure incidence.

2. A secondary cause of the failures was the low value of short transverse fracture toughness at  $-40^{\circ}\text{C}$  for the 7075-T6 material.

3. Fragmentation and stress-corrosion cracking failures of future projectile designs can be minimized by replacing the 7075-T6 material with a lower strength, higher toughness alloy.

4. A notched-bend energy test gave the best indication of failure because it had loading and notch geometry similar to that of the sabot. The tensile test, with no bend loading or notch, gave no indication of failure.

## REFERENCES

1. J. H. Underwood and M. A. Scavullo, "Fracture Behavior of a Uranium or Tungsten Alloy Notched Component With Inertia Loading," Fracture Mechanics: Sixteenth Symposium, ASTM STP 868, (M. F. Kanninen and A. T. Hopper, eds.), American Society for Testing and Materials, Philadelphia, PA, 1985, pp. 554-568.
2. R. J. Bucci, "Selecting Aluminum Alloys to Resist Failure by Fracture Mechanisms," Engineering Fracture Mechanics, Vol. 12, 1979, pp. 407-441.
3. "Standard Test Method for Plane-Strain Fracture Toughness of Metallic Materials, ASTM E-399," 1986 Annual Book of ASTM Standards, Vol. 03.01, American Society for Testing and Materials, Philadelphia, PA, 1986, pp. 522-557.
4. "Standard Methods for Notched Bar Impact Testing of Metallic Materials, ASTM E-23," 1986 Annual Book of ASTM Standards, Vol. 03.01, American Society for Testing and Materials, Philadelphia, PA, pp. 229-253.
5. R. J. Roark and W. C. Young, Formulas for Stress and Strain, McGraw-Hill Book Company, New York, 1975, pp. 564-567.
6. J. H. Underwood and G. S. Leger, "Fracture Toughness of High Strength Steel Predicted from Charpy Energy or Reduction in Area," Fracture Mechanics: Fifteenth Symposium, ASTM STP 833, (R. J. Sanford, ed.), American Society for Testing and Materials, Philadelphia, PA, 1984, pp. 481-498.

TECHNICAL REPORT INTERNAL DISTRIBUTION LIST

	<u>NO. OF COPIES</u>
CHIEF, DEVELOPMENT ENGINEERING DIVISION	
ATTN: SMCAR-CCB-D	1
-DA	1
-DC	1
-DM	1
-DP	1
-DR	1
-DS (SYSTEMS)	1
CHIEF, ENGINEERING SUPPORT DIVISION	
ATTN: SMCAR-CCB-S	1
-SE	1
CHIEF, RESEARCH DIVISION	
ATTN: SMCAR-CCB-R	2
-RA	1
-RM	1
-RP	1
-RT	1
TECHNICAL LIBRARY	5
ATTN: SMCAR-CCB-TL	
TECHNICAL PUBLICATIONS & EDITING SECTION	3
ATTN: SMCAR-CCB-TL	
DIRECTOR, OPERATIONS DIRECTORATE	1
ATTN: SMCWV-OD	
DIRECTOR, PROCUREMENT DIRECTORATE	1
ATTN: SMCWV-PP	
DIRECTOR, PRODUCT ASSURANCE DIRECTORATE	1
ATTN: SMCWV-QA	

NOTE: PLEASE NOTIFY DIRECTOR, BENET LABORATORIES, ATTN: SMCAR-CCB-TL, OF ANY ADDRESS CHANGES.

TECHNICAL REPORT EXTERNAL DISTRIBUTION LIST

	<u>NO. OF COPIES</u>		<u>NO. OF COPIES</u>
ASST SEC OF THE ARMY RESEARCH AND DEVELOPMENT ATTN: DEPT FOR SCI AND TECH THE PENTAGON WASHINGTON, D.C. 20310-0103	1	COMMANDER ROCK ISLAND ARSENAL ATTN: SMCRI-ENM ROCK ISLAND, IL 61299-5000	1
ADMINISTRATOR DEFENSE TECHNICAL INFO CENTER ATTN: DTIC-FDAC CAMERON STATION ALEXANDRIA, VA 22304-6145	12	DIRECTOR US ARMY INDUSTRIAL BASE ENGR ACTV ATTN: AMXIB-P ROCK ISLAND, IL 61299-7260	1
COMMANDER US ARMY ARDEC ATTN: SMCAR-AEE	1	COMMANDER US ARMY TANK-AUTMV R&D COMMAND ATTN: AMSTA-DDL (TECH LIB) WARREN, MI 48397-5000	1
SMCAR-AES, BLDG. 321	1	COMMANDER	
SMCAR-AET-O, BLDG. 351N	1	US MILITARY ACADEMY	1
SMCAR-CC	1	ATTN: DEPARTMENT OF MECHANICS	
SMCAR-CCP-A	1	WEST POINT, NY 10996-1792	
SMCAR-FSA	1		
SMCAR-FSM-E	1	US ARMY MISSILE COMMAND	
SMCAR-FSS-D, BLDG. 94	1	REDSTONE SCIENTIFIC INFO CTR	2
SMCAR-IMI-I (STINFO) BLDG. 59	2	ATTN: DOCUMENTS SECT, BLDG. 4484	
PICATINNY ARSENAL, NJ 07806-5000		REDSTONE ARSENAL, AL 35898-5241	
DIRECTOR US ARMY BALLISTIC RESEARCH LABORATORY ATTN: SLCBR-DD-T, BLDG. 305	1	COMMANDER US ARMY FGN SCIENCE AND TECH CTR ATTN: DRXST-SD 220 7TH STREET, N.E. CHARLOTTESVILLE, VA 22901	1
ABERDEEN PROVING GROUND, MD 21005-5066			
DIRECTOR US ARMY MATERIEL SYSTEMS ANALYSIS ACTV ATTN: AMXSY-MP	1	COMMANDER US ARMY LABCOM MATERIALS TECHNOLOGY LAB ATTN: SLCMT-IML (TECH LIB)	2
ABERDEEN PROVING GROUND, MD 21005-5071		WATERTOWN, MA 02172-0001	
COMMANDER HQ, AMCCOM ATTN: AMSMC-IMP-L	1		
ROCK ISLAND, IL 61299-6000			

NOTE: PLEASE NOTIFY COMMANDER, ARMAMENT RESEARCH, DEVELOPMENT, AND ENGINEERING CENTER, US ARMY AMCCOM, ATTN: BENET LABORATORIES, SMCAR-CCB-TL, WATERVLIET, NY 12189-4050, OF ANY ADDRESS CHANGES.

TECHNICAL REPORT EXTERNAL DISTRIBUTION LIST (CONT'D)

	<u>NO. OF COPIES</u>		<u>NO. OF COPIES</u>
COMMANDER US ARMY LABCOM, ISA ATTN: SLCIS-IM-TL 2800 POWDER MILL ROAD ADELPHI, MD 20783-1145	1	COMMANDER AIR FORCE ARMAMENT LABORATORY ATTN: AFATL/MN EGLIN AFB, FL 32542-5434	1
COMMANDER US ARMY RESEARCH OFFICE ATTN: CHIEF, IPO P.O. BOX 12211 RESEARCH TRIANGLE PARK, NC 27709-2211	1	COMMANDER AIR FORCE ARMAMENT LABORATORY ATTN: AFATL/MNF EGLIN AFB, FL 32542-5434	1
DIRECTOR US NAVAL RESEARCH LAB ATTN: MATERIALS SCI & TECH DIVISION CODE 26-27 (DOC LIB) WASHINGTON, D.C. 20375	1 1	METALS AND CERAMICS INFO CTR BATTELLE COLUMBUS DIVISION 505 KING AVENUE COLUMBUS, OH 43201-2693	1

NOTE: PLEASE NOTIFY COMMANDER, ARMAMENT RESEARCH, DEVELOPMENT, AND ENGINEERING CENTER, US ARMY AMCCOM, ATTN: BENET LABORATORIES, SMCAR-CCB-TL, WATERVLIET, NY 12189-4050, OF ANY ADDRESS CHANGES.